Brief Survey of High Speed Flow Control Using Microwave Energy Deposition

Doyle D. Knight
Department of Mechanical and Aerospace Engineering
Rutgers - The State University of New Jersey
New Brunswick, New Jersey 08901 USA

Abstract

Although microwave discharges in air have been studied for decades, their application to aerodynamic flow control in supersonic flows has only recently been examined in depth. In this paper, a brief survey of several papers from 2001 to 2006 is presented.

1. Introduction

Electromagnetic Local Flow Control (ELFC) comprises a wide range of energy deposition techniques including DC discharge, Dielectric Barrier Discharge (DBD), electron beam, laser and microwave. In recent years there has been intense activity in developing fundamental understanding and practical applications of ELFC for aerodynamic applications. Recent surveys include Zheltovodov,[1] Knight et al,[2] Knight,[3] Fomin et al[4] and Bletzinger et al.[5] ELFC has several potential advantages compared to conventional mechanical and electro-mechanical techniques including virtually instantaneous activation time, action-at-a-distance and capability for tailoring the energy deposition to achieve the desired flow control.

2. Survey

This paper surveys selected recent experimental and theoretical research on microwave energy deposition in air. The paper summarizes the results of a series of papers from 2001 in chronological order. The focus of the survey is aerodynamic effects, and consequently omits discussion of the details of the microwave plasma.

2.1 Kolesnichenko et al 2001

Kolesnichenko et al[6] performed a pioneering set of experiments to examine the effect of a microwave energy pulse in air (and other gases) on the drag of a blunt cylinder at Mach 1.7 for ambient pressure $p_\infty = 60$ Torr and temperature $T_\infty = 200$ K. Single microwave pulses at 9 GHz with peak power $P = 210$ kW and typical duration $\tau = 1.2\mu$s to 2.2μs were focused upstream of the blunt body shock. Both linear and circularly polarized electric field E were considered. Typical measured electric field strength E along the $x-$axis (streamwise) is shown in Fig. 1 for linearly polarized electric field (along the $y-$axis). A typical range of values for the reduced field E/N (where N is the particle concentration) is 80 to 110 Townsend (Fig. 2).

Multiple plasmoids (typically, up to three) are generated by the single microwave pulse. The average velocity of each plasmoid is approximately the freestream velocity (Fig. 3). Schlieren images of the interaction of the plasma with the blunt body shock are shown in Figs. 5 and 6 corresponding to $t = 6\mu$s and 21μs after the microwave pulse. In the former image, the plasmoid has not yet reached the blunt body shock, whereas in the latter image the interaction of the plasmoid with the blunt body shock is evident in the distortion of the shock wave. This interaction causes a significant reduction in the surface pressure as indicated in Fig. 4, thereby resulting in a momentary decrease in frontal drag. The explanation for this phenomenon is given in Subsection 2.6.

2.2 Kolesnichenko et al 2002

Kolesnichenko et al[7] presented a series of unsteady Euler simulations of the interaction of a heated channel (denoted a “density well”) with a two-dimensional blunt body at $M_\infty = 1.9$. The heated channel represents a single microwave

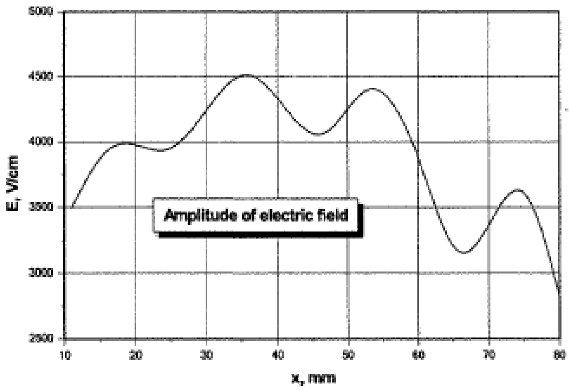

Figure 1: Typical E field *vs* x

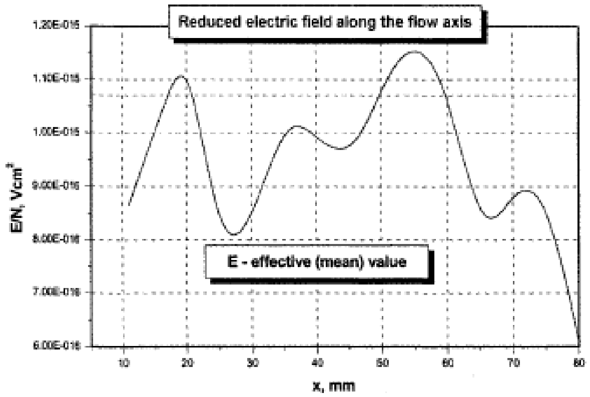

Figure 2: Typical E/N field *vs* x

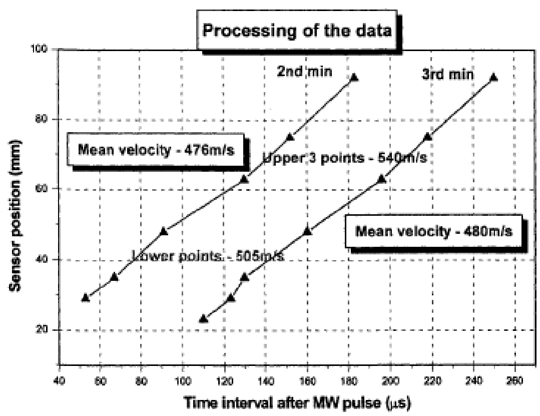

Figure 3: Plasmoid position *vs* t

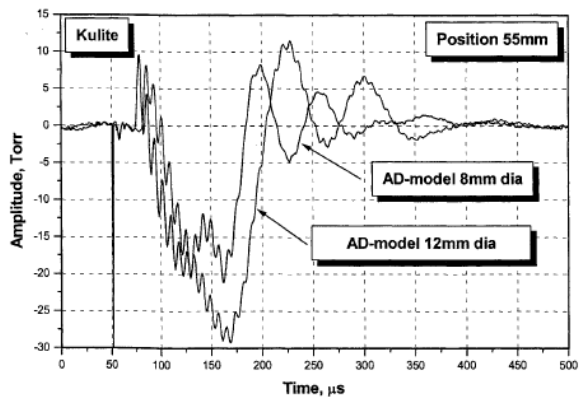

Figure 4: p *vs* t

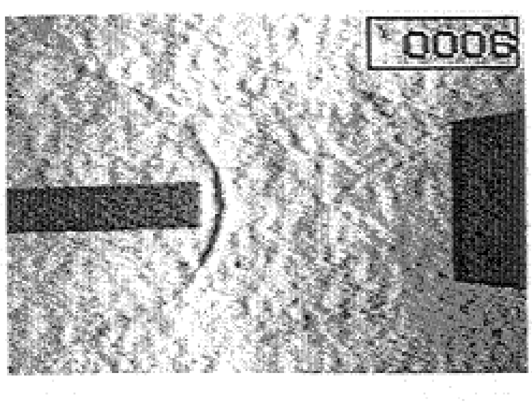

Figure 5: Schlieren image ($t = 6\mu$s)

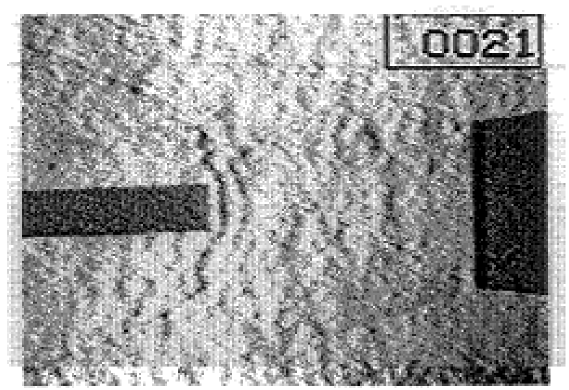

Figure 6: Schlieren image ($t = 21\mu$s)

filament and was assumed to be aligned in the streamwise direction on the body centerline. Fig. 7 displays the computed Schlieren images at four instants of time. The first image shows the lensing forward of the blunt body shock due to the initial interaction with the heated channel. The second and third images display the formation of a vortex pair and recirculation region, and the fourth image shows the reflected shock wave. The computed surface pressure on the centerline is displayed in Fig. 8. The initial pressure drop in Phase I is associated with the expansion wave generated by the interaction of the heated channel with the blunt body shock. In Phase II, the vortex formation leads to a significant decrease in surface pressure associated with the momentary effective streamlining of the body due to the creation of the recirculation region immediately ahead of the body. In Phase III, the vortex is convected downstream and the surface pressure recovers to its undisturbed level in Phase IV. These features are in agreement with the experimental measurements shown in Fig. 4.

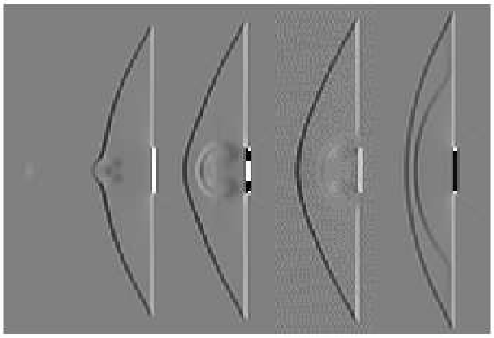

Figure 7: Schlieren images

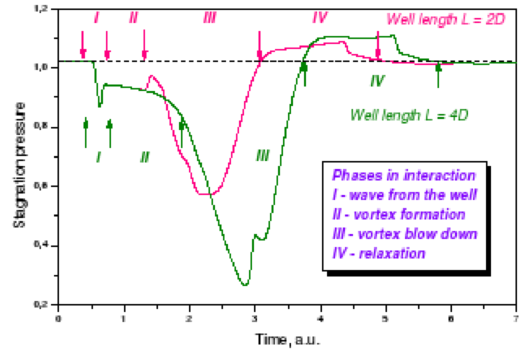

Figure 8: *p vs t*

2.3 Kolesnichenko et al 2003

Kolesnichenko et al[8] developed a model for the formation of the thin hot channels in microwave discharge in air. The analytic model yields a finite time collapse-like creation of a hot plasma channel with high electron concentration and temperature. The formation time of the hot channel is

$$t_{\text{channel}} = \left[1.5k^2\eta\sigma_o E_o^2 \rho_o^{-1}\right]^{-1/3} \tag{1}$$

where k is proportional to the microwave wavenumber, η is the fraction of the dissipated energy transformed into heating of the gas, σ_o is the conductivity, E_o is the amplitude of the electric field and ρ_o is the ambient density. For typical values (σ_o = 100 Siemens, λ = 3 cm, p_o = 76 Torr, E_o = 3 kV/cm), the model predicts $t_{\text{channel}} \approx 1\mu$s in agreement with experiment.

2.4 Mashek et al 2004

Mashek et al[9] conducted experiments to ascertain the capability of a laser spark to act as a precursor ("initiator") for microwave discharge in air at atmospheric pressure. The experimental configuration is shown in Fig. 9. A ruby laser (694.3 nm, 220 mJ pulse maximum, 25 ns pulse duration maximum) is focused in air at atmospheric pressure. The microwave generator has a peak power of 180 kW and a typical pulse duration 1.2μs. The effect of different delay times between the laser and microwave pulses was investigated, and a maximum luminosity of the microwave discharge was observed for a delay of 80μs to 110μs. A Schlieren image is shown in Fig. 10. The focus of the laser pulse is indicated by the bright spot. The outer circle is the blast wave originating from the laser pulse. The next inner semi-circle is the reflection of the blast wave from the parabolic microwave mirror. The innermost circle is the blast wave generated by the microwave discharge. This preliminary study demonstrated the potential for laser spark initiation of microwave discharge at atmospheric pressure.

2.5 Brovkin et al 2006

Brovkin et al[10] performed a series of experiments to evaluate quantitatively the effect of a laser spark precursor on the breakdown voltage required for microwave energy deposition in air at subatmospheric to atmospheric pressure. The experimental configuration is shown in Fig. 11. A Nd:YAG laser (532 nm, 130 mJ/pulse maximum, 10 ns pulse duration maximum) is focused in air at atmospheric or subatmospheric pressure to generate a plasma as an initiator for a microwave discharge. The microwave generator has a maximum power 700 kW operating at 13 GHz. The electric fields of the laser and microwave are mutually perpendicular. An example of the microwave discharge following a laser spark precursor is shown in Fig. 12. The pulse power required for the laser spark generation in quiescent air as a function of ambient pressure is shown in Fig. 13 and varies from approximately 105 mJ at 70 Torr to 20 mJ at 750 Torr. The laser spark precursor enables a microwave discharge at atmospheric pressure as indicated in Fig. 14, and the required microwave field decreases with increasing laser pulse energy. These results imply the potential for creating microwave discharges at arbitrary locations in the vicinity of an aerodynamic body.

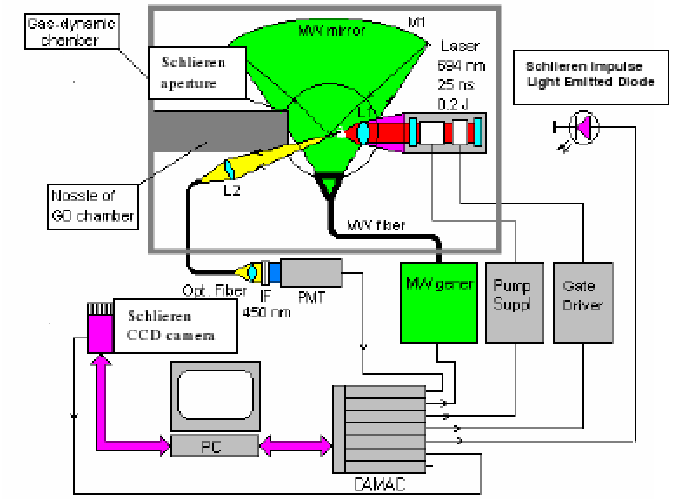

Figure 9: Experiment

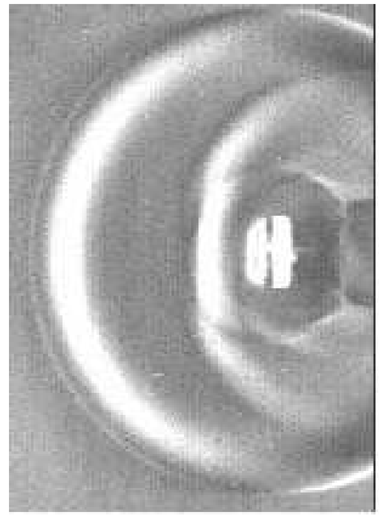

Figure 10: Schlieren

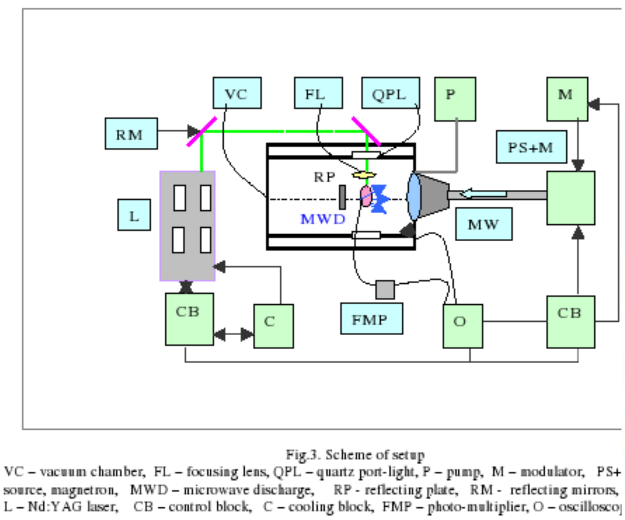

Figure 11: Experiment

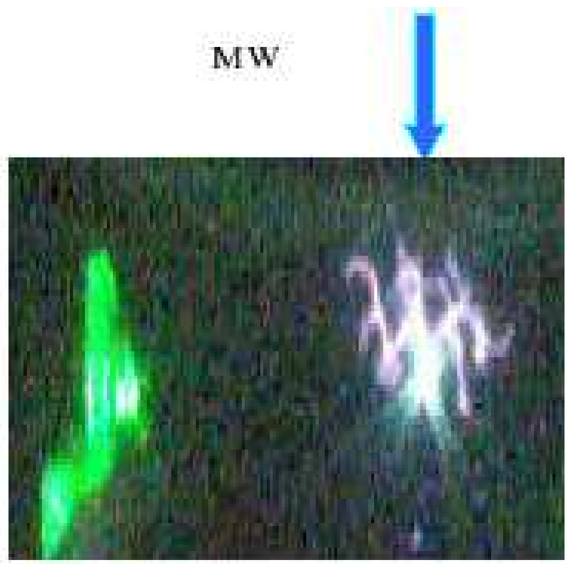

Figure 12: MW discharge after laser pulse

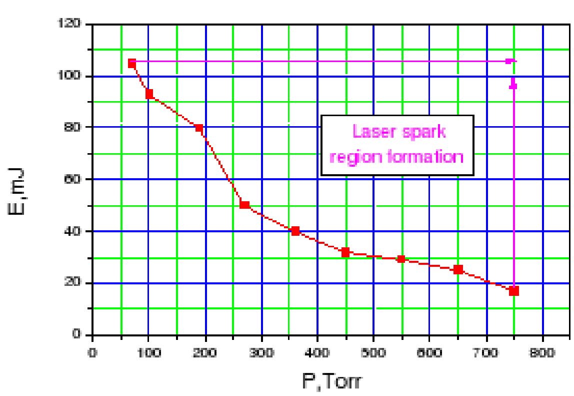

Figure 13: Laser spark threhold energy

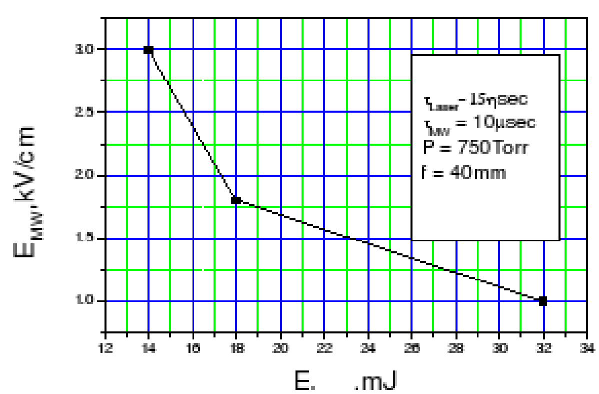

Figure 14: Effect of laser precursor on MW

2.6 Efficiency

The efficiency of steady energy deposition for drag reduction can be examined in two limiting cases. First, consider the situation wherein the cross section of the region of energy deposition A_∞ is comparable or larger than cross section A of the aerodynamic body. The power required to overcome the drag on the body is

$$P = \frac{1}{2} C_D \rho u^2 A U_\infty \tag{2}$$

where ρ and u are the effective density and velocity upstream of the body due to the energy deposition, A is the cross-sectional area of the body and U_∞ is the freestream body. We may define the efficiency of energy deposition as

$$\eta = -\frac{dP}{dQ} \tag{3}$$

where $dQ = \rho_\infty U_\infty A_\infty dq$ with A_∞ the cross-sectional area of the energy deposition region and q is the energy added per unit mass per unit time. Since the drag coefficient C_D is relatively constant for blunt bodies in supersonic flow,

$$\frac{dP}{dQ} = \frac{1}{\dot{m}} \frac{C_D}{2} A U_\infty \frac{d\rho u^2}{dq} \tag{4}$$

where $\dot{m} = \rho_\infty U_\infty A_\infty$. For Rayleigh flow (assuming the flow is not choked),

$$\frac{d\rho u^2}{dq} = -\frac{\rho u^2}{(M^2 - 1)\, c_p T} \tag{5}$$

Approximating $T \approx T_\infty$ and $\rho \approx \rho_\infty$,

$$\eta = \frac{(\gamma - 1)}{2} C_D \frac{A}{A_\infty} \frac{M_\infty^2}{\left(M_\infty^2 - 1\right)} \tag{6}$$

Typically, $C_D \approx 1$ for blunt bodies[1]. The foregoing analysis applies to $A_\infty \geq A$, and thus, the estimated maximum efficiency $\eta \approx \frac{1}{2}(\gamma - 1) = 0.7$ for air. Therefore, energy deposition into a region whose cross-sectional area is comparable to the body cross-sectional area is ineffective, *i.e.*, the savings in power due to the reduction in drag is less than the power required to heat the gas.

Second, consider the situation wherein the cross section of the energy deposition A_∞ is small comparable to the cross section A of the aerodynamic body. Assume for simplicity that the energy deposition occurs at constant pressure (isobaric) and in a cylindrical region of diameter d (a "filament") and streamwise length L aligned with the flow (with $d \ll L$, and hence the terminology "filament") and initially located upstream of the blunt body. The net energy ΔE_f added in the volume $A_\infty L$ to increase the temperature from the ambient T_∞ to the level $T_f = T_\infty + \Delta T$ is

$$\Delta E_f = A_\infty L c_p \rho_f \Delta T \tag{7}$$

where ρ_f is the density of the filament. Since the energy is assumed added at constant pressure,

$$\Delta E_f = A_\infty L c_p \frac{p_\infty}{R} (1 - \alpha) \tag{8}$$

where R is the gas constant for air and $\alpha = \rho_f / \rho_\infty$. During the interaction time τ of the filament with the aerodynamic body, the net energy savings ΔE_d due to decrease in frontal drag is

$$\Delta E_d = U_\infty I^* \tag{9}$$

where $I*$ is the impulse

$$I^* = \int_o^\tau \int_A (p - p_o)\, dA\, dt \tag{10}$$

where p is the instantaneous pressure on the frontal surface of the body during the interaction, p_o is the (steady) pressure on the frontal surface of the body in the absence of the interaction, and dA is the projected elemental area of the front surface. Define the non-dimensional impulse I according to

$$I = \frac{I*}{p_s A L U_\infty^{-1}} \tag{11}$$

[1] For example, the drag coefficient for a sphere[11] is $0.92 \leq C_D \leq 1.0$ for $1.5 \leq M_\infty \leq 4.0$.

where p_s is the stagnation pressure downstream of a normal shock at the freestream Mach number M_∞ (Rayleigh pitot formula). Assuming the aerodynamic body is cylindrical with diameter D, the efficiency $\eta = \Delta E_d / \Delta E_f$ is

$$\eta = \left[\frac{(\gamma+1)}{2} M_\infty^2\right]^{\gamma/(\gamma-1)} \left[\frac{\gamma+1}{2\gamma M_\infty^2 - (\gamma-1)}\right]^{1/(\gamma-1)} \frac{(\gamma-1)}{\gamma} \left(\frac{D}{d}\right)^2 \frac{I}{(1-\alpha)} \tag{12}$$

For $M_\infty \gg 1$,

$$\eta \sim 0.37 M_\infty^2 \left(\frac{D}{d}\right)^2 \frac{I}{(1-\alpha)} \tag{13}$$

Unlike the first situation, the efficiency improves both with increasing Mach number M_∞ and area ratio (D/d). Indeed, if we conjecture that the impulse I is relatively insensitive to (D/d), the efficiency increases dramatically with decreasing filament diameter. Numerical simulations[7] confirm this conjecture.

3. Conclusions

Microwave energy deposition has been shown experimentally to achieve drag reduction for blunt bodies in supersonic flow. Experimental imaging shows that the principal mechanism is the interaction of the high temperature channels (filaments) with the blunt body shock resulting in the aerodynamic streamlining of the body through creation of a recirculation region. Numerical simulations using the Euler equations are in agreement with experiment.

References

[1] Zheltovodov, A. Development of the Studies on Energy Deposition for Application to the Problems of Supersonic Aerodynamics. Preprint No. 10-2002, Khristianovich Institute of Theoretical and Applied Mechanics, Novosibirsk, Russia, 2002.

[2] Knight, D., Kuchinskiy, V., Kuranov, A., and Sheikin, E. Survey of Aerodynamic Flow Control at High Speed Using Energy Addition. AIAA Paper No. 2003-0525, January 2003.

[3] Knight, D. Survey of Magneto-Gasdynamic Local Flow Control at High Speeds, AIAA Paper No. 2004-1191, 2004.

[4] Fomin, V., Tretyakov, P. and Taran, J.-P. Flow Control Using Various Plasma and Aerdynamic Approaches (Short Review). *Aerospace Science and Technology*, 8:411–421, 2004.

[5] Bletzinger, P., Ganguly, B., VanWie, D. and Garscadden, A. Plasmas in High Speed Aerodynamics. *Journal of Physics D: Applied Physics*, 38:R33-R57, 2005.

[6] Kolesnichenko, Y., Brovkin, V., Leonov, S., Krylov, A., Lashkov, V., Mashek, I., Gorynya, A. and Ryvkin, M. Investigation of AD-Body Interaction with Microwave Discharge Region in Supersonic Flow. AIAA Paper No. 2001-0345, January 2001.

[7] Kolesnichenko, Y., Brovkin, V., Azarova, O., Grudnitsky, V., Lashkov, V. and Mashek, I. Microwave Energy Release Regimes for Drag Reduction in Supersonic Flows. AIAA Paper No. 2002-0353, January 2002.

[8] Kolesnichenko, Y., Brovkin, V., Khmara, D., Lashkov, V., Mashek, I. and Ryvkin, M. Fine Structure of MW Discharge: Evolution Scenario. AIAA Paper No. 2003-0362, January 2003.

[9] Mashek, I., Anisimov, Y., Lashkov, V., Kolesnichenko, Y., Brovkin, V. and Rivkin, M. Microwave Discharge Initiated by Laser Spark in Air. AIAA Paper No. 2004-0358, January 2004.

[10] Brovkin, V., Afanas'ev, S., Khmara, D. and Kolesnichenko, Y. Experimental Investigation of Combined Laser-DC-MW Discharges. AIAA Paper No. 2006-1459, January 2006.

[11] Charters, A. and Thomas, R. The Aerodynamic Performance of Small Spheres from Subsonic to High Supersonic Velocities. *Journal of the Aeronautical Sciences*, 12:468, October 1945.

This page has been purposedly left blank